JSS Focus Issue on Gallium Oxide Based Materials and Devices

^{60}Co Gamma Ray Damage in Homoepitaxial β-Ga_2O_3 Schottky Rectifiers

Jiancheng Yang,[1] Gregory J. Koller,[1] Chaker Fares,[1] F. Ren,[1,*] S. J. Pearton,[2,*,z] Jinho Bae,[3] Jihyun Kim,[3] and David J. Smith[4]

[1]*Department of Chemical Engineering, University of Florida, Gainesville, Florida 32611, USA*
[2]*Department of Materials Science and Engineering, University of Florida, Gainesville, Florida 32611, USA*
[3]*Department of Chemical and Biological Engineering, Korea University, Anam-dong, Sungbuk-gu, Seoul, Korea*
[4]*Department of Physics, Arizona State University, Tempe, Arizona 85287, USA*

β-Ga_2O_3 Schottky rectifiers consisting of thick (10 μm) epitaxial drift regions on conducting substrates are shown to have a high tolerance to ^{60}Co gamma ray irradiation. This is due to the low carrier removal rate of <1 cm^{-1} for gamma rays, which contrasts to values of 300–500 cm^{-1} for MeV protons and alpha particles in the same rectifier structures. Changes in diode ideality factor, Schottky barrier height, on-resistance, on-off ratio, and reverse recovery time are all minimal for fluences up to 2 × 10^{16} cm^{-2} (absorbed dose of 100 kGy (Si)). These results are consistent with previous reports on gamma-irradiation of Ga_2O_3 metal oxide semiconductor field effect transistors (MOSFETs) where changes were ascribed to damage in the gate dielectric and not to the Ga_2O_3 itself.

 [DOI: 10.1149/2.0091907jss]

Manuscript submitted November 19, 2018; revised manuscript received February 7, 2019. Published February 13, 2019. *This paper is part of the JSS Focus Issue on Gallium Oxide Based Materials and Devices.*

The effects of gamma ray irradiation on wide bandgap semiconductors are much less pronounced than for proton, electron, or neutron irradiation of these same materials.[1–14] In the case of SiC, the effective carrier removal rates normalized to non-ionizing energy loss for gamma rays are up to 6 orders of magnitude less than for alpha particles and approximately two orders of magnitude lower than for electrons and neutrons.[1–4] There was less degradation in Metal Oxide Semiconductor (MOS) transistors than metal-based gate devices, indicating that the gate oxide is a key determinant of the changes due to gamma ray exposure.[4] Similar trends in terms of carrier removal rate are obtained for the case of GaN-based High Electron Mobility Transistors (HEMTs) exposed to these same forms of radiation.[4–14] However, in that case, there was no difference in the degree of device degradation between MOS gate and metal gate devices. The changes reported for gamma-irradiated AlGaN/GaN HEMTs often show inconclusive results in the sense that improvement as well as degradation in the GaN material and devices have been reported. Lee et al.[11] reported that low absorbed doses of gamma irradiation (<300 Gy) have a tendency to improve AlGaN/GaN HEMT device characteristics, while high absorbed doses (>300 Gy) lead to device degradation. The absorbed dose (dE/dM) is the mean energy (dE) imparted per unit mass (dM) and is specified in terms of a standard material such as Si or SiO_2. The unit of absorbed dose is the Gy. The fluence is the number of gamma rays passing through the medium, with units of cm^{-2}.

Compensation and re-structuring of defects/traps has been also reported by Vitusevich et al.,[13] with cathodoluminescence showing improvements in the interface properties of AlGaN/GaN heterostructures for absorbed γ irradiation doses of 10 kGy. Hwang et al.[14] reported increases in both drain current and electron mobility for doses up to 700Gy. Gamma-ray interactions with semiconductors differ from those with charged particles, where the energy loss mechanisms are due to atomic collisions (non-ionizing energy loss or NIEL, also referred to as displacement damage) or ionization. The displacement defects typically have energy states in the bandgap, which significantly influence the electrical properties of semiconductor devices. In the case of gamma rays, photon interactions can lead to Compton scattering, photoelectric effect, and electron-hole pair production. Since gamma rays produce energetic secondary electrons, these can also cause displacement damage. ^{60}Co gamma-rays provide advantages in radiation studies since the created defects are uniformly distributed throughout the sample, no secondary irradiation is induced, and the samples can be safely handled immediately after the irradiation.[15–20]

Beyond the most common wide bandgap semiconductors discussed above, there is increasing interest in the radiation hardness of Ga_2O_3.[21–25] In the only previous report to date on gamma irradiation, Wong et al.[25] irradiated lateral depletion-mode β-Ga_2O_3 (010) metal oxide semiconductor field effect transistors (MOSFETs) to a cumulative γ-ray dose of 1.6 MGy (SiO_2) and saw a change in the carrier concentration of ∼4%, confirming that only a small concentration of radiation-induced bulk defects were generated in the Ga_2O_3 channel. The changes in maximum drain-source current and transconductance were <5%, however the drain-source current (I_{DS}) on/off ratios did exhibit a reduction by up to two orders of magnitude. This reduction was ascribed to damage to the Al_2O_3 gate dielectric and additional interface charge trapping, with an increase in interfacial trap density of 10–20%.[25] A conclusion of this work was that the degradation of gate oxide properties was mainly responsible for the changes upon gamma ray irradiation, as has been reported for a comparison of SiC MOSFETs versus MESFETs[4] and that the device fabrication process was critical in determining radiation tolerance.

In this paper we examine the effect of ^{60}Co γ-ray damage on Ga_2O_3 rectifiers. Since these are simple two terminal devices that do not involve gate dielectrics, they are a direct test of the intrinsic radiation hardness of the Ga_2O_3 and enable a comparison of carrier removal rates to proton, electron, and alpha particle irradiation of the same rectifier structures. In the case of GaN HEMTs, the performance of the devices relies on preserving the heterointerface that controls carrier density and mobility in the channel. Use of a simple, metal-gate, thick epitaxial vertical rectifier eliminates the variables due to gate oxides and heterointerfaces.

Experimental

The Schottky rectifiers shown in Figure 1 were used in these experiments. Full area back ohmic contacts of Ti/Au and front-side Ni/Au Schottky contacts (100 μm diameter) were fabricated on a structure consisting of 10 μm thick, Si-doped (2–3 × 10^{16} cm^{-3}) epitaxial Ga_2O_3 grown by Halide Vapor Phase Epitaxy on conducting (Sn-doped, 9 × 10^{18} cm^{-3}), (001) substrates that were 0.65 mm thick.

*Electrochemical Society Fellow.
zE-mail: spear@mse.ufl.edu

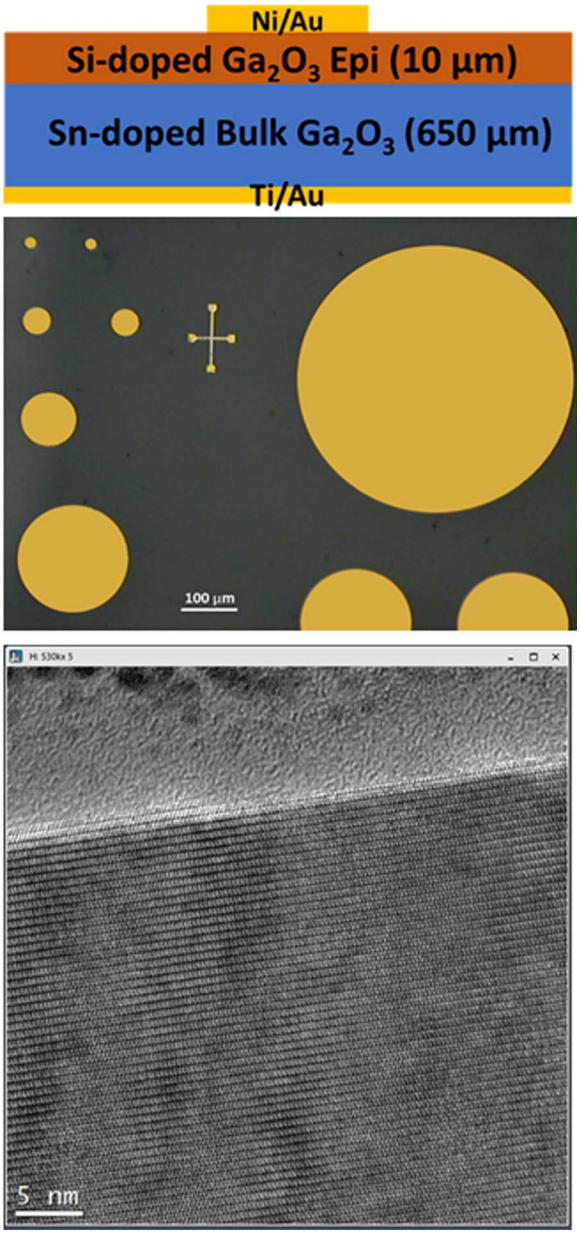

Figure 1. Schematic of rectifier structure used in these experiments (top), plan view of contact layout (center) and high resolution TEM of the upper section of the HVPE layer (bottom). The bright lines shows the surface of the epi layer.

The growth temperature was 650°C, with a HCl percentage of total flow ∼0.4%, HCl-to-O_2 ratio of 0.25 and the growth rate was around 15 nm.min^{-1}. The chlorine concentration in the epi layers was $<10^{16}$ cm^{-3}. The X-Ray Diffraction full-width-half-maximum was <350 arc.sec for the substrate.[26] Cross-sectional transmission electron microscopy showed excellent quality of the homoepitaxy, as shown at the bottom of Figure 1. More details of the HVPE growth process are given elsewhere.[26–30]

A ^{60}Co source with photon energies of 1.33 and 1.17 MeV was used for gamma irradiation. The decay diagram of ^{60}Co diagram in Figure 2 shows the main energies of gamma-photons and beta-particles emitted. ^{60}Co gamma-ray irradiation was performed cumulatively from a dose of 1–100 kGy (Si) in air ambient at the Korea Atomic Energy Research Institute (KAERI). The gamma-ray source was kept in water (source storage pool) before the irradiation experiments. The distance from the gamma-ray source to the sample was approximately 19 cm. The average dose rate was 23.54 kGy/hr (Si) in ambient air, measured

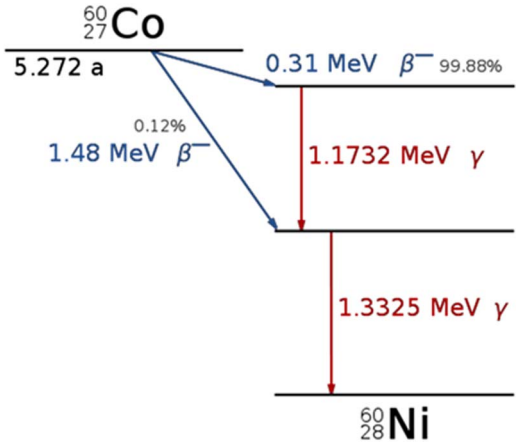

Figure 2. Cobalt-60 decay diagram.

by a series of dosimeters that obtain the absorbed energy and energy by a dE/dx measurement. The sample will heat up during the γ-ray irradiation,[31–33] according to $H\gamma \cong 1.6 \times 10^{-13} Eave.\varphi_{\gamma in}$, where, Hγ is the heating rate, Ea*ve* is average energy of photons in MeV and $\varphi_{\gamma in}$ is the incident photon flux density. Using this equation, a maximum temperature of ∼130°C would be reached for the highest dose utilized in this study without thermal coupling. This expected temperature rise is consistent with changes seen in the ceramic packaging material. The rectifier performance was characterized using an Agilent 4156 parameter analyzer.

Results and Discussion

Figure 3 shows there was no measurable change in forward current-voltage (I-V) characteristics, even after the highest dose of 100 kGy (Si). We used the usual thermionic emission model to extract the Schottky barrier height (Φ_B), on-state resistance (R_{ON}) and ideality factor (n) from these characteristics. The Schottky barrier height, diode ideality factor and reverse breakdown voltage (defined as the voltage at which the reverse current was 1µA.cm^{-2}) were basically unchanged, as shown in Table I. This indicates that the amount of damage introduced was small enough that it did not affect the dominant current transport mechanism of thermionic emission under these conditions. The capacitance-voltage characteristics were also obtained and are shown in Figure 4 (top). The drift region carrier concentration extracted from the C^{-2}-V plot is shown at the bottom of Figure 4 and the differences caused by irradiation shown in Table I. The changes

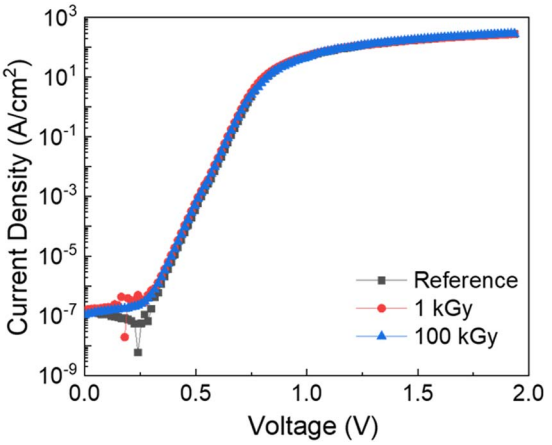

Figure 3. Forward current density-voltage plots before and after gamma irradiation at different doses.

Table I. Summary of Ga_2O_3 rectifier performance before and after exposure to absorbed doses of 1 or 100 kGy(Si), equivalent to doses of 2×10^{14} or 2×10^{16} cm^{-2}.

Parameter	Un-irradiated	Dose 2×10^{14} cm^{-2}	Dose 2×10^{16} cm^{-2}
Barrier Height(eV)	1.09	1.03	1.04
Ideality Factor	1.06	1.10	1.10
R_{ON} ($m\Omega.cm^{-2}$)	3.7	3.7	3.7
Drift Region Carrier Concentration (10^{16} cm^{-3})	1.14 ± 0.05	1.12 ± 0.04	1.10 ± 0.03
Change in Drift Region Carrier Concentration (10^{14} cm^{-3})	n/a	1.01 ± 0.5	1.41 ± 0.2
Reverse Breakdown Voltage(V)	1845 ± 15	1850 ± 15	1838 ± 15
Carrier Removal Rate (cm^{-1})	n/a	0.5 ± 0.2	0.007 ± 0.001
On/off ratio (−10 V)	4.5×10^8	7.8×10^8	6.3×10^8
Reverse Recovery Time (ns)	18.5	18.5	18.5

again were small, of order 10^{14} cm^{-3}, which has little impact on the drift region doped at 10^{16} cm^{-3}. This leads to the small carrier removal rates, defined as the change in carrier density divided by fluence. As pointed out earlier, since gamma rays can produce secondary electrons, these electrons cause the displacement damage through non-ionizing energy loss (NIEL).[33,34] Compton-scattering of the main ^{60}Co gamma-photons lines, at 1.17 MeV and 1.33 MeV, create a significant density of low energy photons ($E\gamma \leq 0.60$ MeV). These Compton electrons cause the generation of Frenkel pairs and defect clusters.[32–34] Some of these defects can migrate and recombine or create complexes, which are stable even at room temperature.[33,34]

To calculate average gamma-NIEL, the differential electron flux containing Compton and photovoltaic electrons has to be evaluated. The gamma-ray fluence can be calculated from the total ionizing dose using the relation 1rad (Si) = 2.0×10^9 photons/cm^2.[31] The concentration of point defects introduced via displacement damage can be expressed in terms of an effective Frenkel-pair generation rate per incident gamma-rays photon[33,34]

$$N_F = N_D.\sigma_d.\varphi_\gamma$$

where N_F is the concentration of generated Frenkel-pairs, $N_D.\sigma_d$ is the effective defect production rate, σ_d is the effective displacement cross section, and N_D is the number of lattice atoms per unit volume.

Carrier removal rates were calculated by dividing the change in carriers between the irradiated devices and their references by the gamma fluence used to irradiate them.[3,35–39] This is represented as $N_\varphi = N_0 - k\varphi$[23], where N_φ is the irradiated carrier concentration, N_O is the non-irradiated carrier concentration, φ is the gamma fluence, and k is the carrier removal rate. The carrier concentrations were calculated from capacitance voltage measurements using the following equation: $N(W_D) = \frac{2}{q\varepsilon_0\varepsilon_r A^2}[-\frac{1}{d(1/C_D^2)/dV}]$[24]. The slope of the inverse squared capacitance against voltage, along with the contact area and dielectric constant of Ga_2O_3 (the value of 10.2 was reported by Passlack et al.[36]), was used to calculate the carrier concentrations. The gamma fluences were calculated using the gamma dose, irradiation energy, and the mass-energy absorption coefficient for Ga_2O_3. This is represented by the equation: $\varphi_g = \frac{D_g}{E_g \mu}$.[3] The mass-energy absorption coefficient for Ga_2O_3 was calculated by a weighted average of the mass-energy coefficients for the individual elements: $\frac{\mu}{\rho} = \sum_i w_i(\frac{\mu}{\rho})_i$.[38] The mass-energy coefficients for gallium and oxygen were 0.02371 and 0.02669 $\frac{cm^2}{g}$,[35] respectively and are based from a 1.25 MeV irradiation energy.

Figure 5 shows a compilation of carrier removal rates in Ga_2O_3 for different types and energies of radiation. Note that the values for gamma rays are <1 and are several orders of magnitude lower than

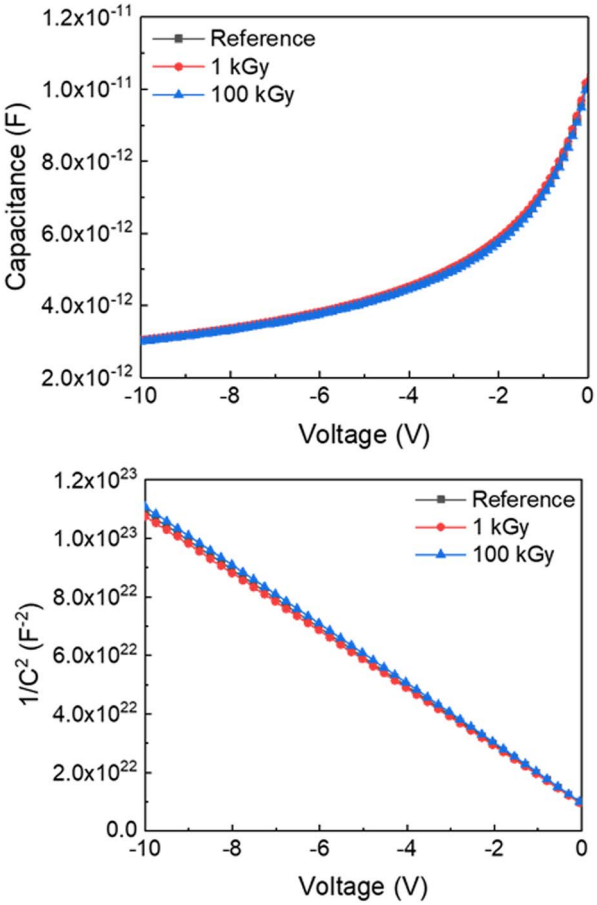

Figure 4. Capacitance-voltage (top) and C^{-2}-V plot (bottom) before and after gamma irradiation at different doses.

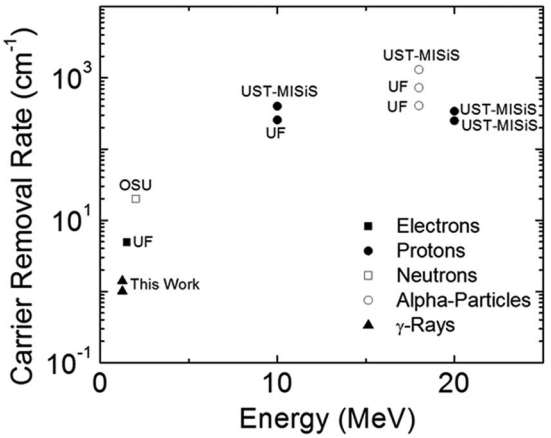

Figure 5. Carrier removal rates in Ga_2O_3 for different types of radiation, as a function of energy. Note that the units of carrier removal rate are per particle and not temporal units. The results for electrons are from Ref. 52, the neutron data from Ref. 23, the alpha particle data from Ref. 47 (UF) and 45(UST MiSIS) and the proton results from refs.50 (UF), 45 and 46 (UST MiSIS).

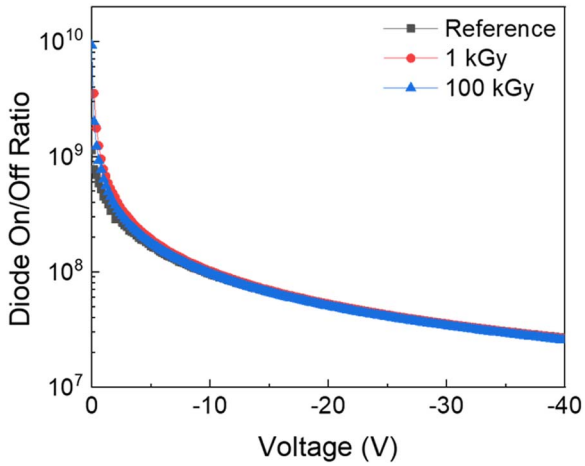

Figure 6. Diode on/off ratio as a function of voltage before and after gamma irradiation.

for protons and a factor of 5–10 lower than for neutrons and electrons. In addition, the data reported to date shows that the carrier removal rates in Ga_2O_3 are basically comparable to those reported previously for GaN.[40–43] It should be noted that carrier removal rates for GaN were measured in High Electron Mobility Transistor structures, which have much thinner layers than the rectifier structures used here for Ga_2O_3 and so direct comparisons should be avoided, but one generally finds that the range of carrier removal rates in GaN for each of the different radiation types are similar within a factor of 30–50% of the values obtained for the same radiation types in Ga_2O_3 = under similar doses rates and total fluences. These results reiterate that Ga_2O_3 is a radiation-hard semiconductor, in line with the expectation from its high atomic binding energies.[44–52]

The on-off ratio for a rectifier is a sensitive measure of radiation damage. Figure 6 shows that there was no measurable change in this ratio for the highest gamma ray dose for conditions where the rectifier was switched from 1V forward bias to different negative (reverse) bias voltages. This is in sharp contrast to the case of electron irradiation of these same types of rectifiers, where the on/off ratio at −10V reverse bias voltage was severely degraded after radiation, decreasing from $\sim 10^7$ in the reference diodes to $\sim 2 \times 10^4$ after an electron fluence of 1.43×10^{16} cm^{-2}.[52] Finally, the reverse recovery time of ~18 ns was unchanged by the gamma irradiation, as shown in Figure 7. If there were significant lattice disorder created, the lifetime should decrease since carrier lifetime would be degraded.

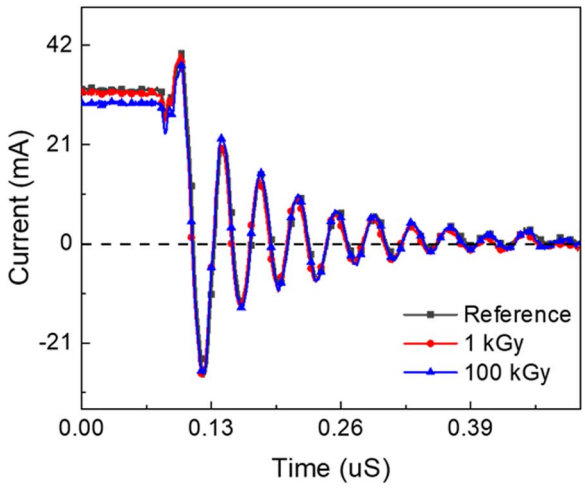

Figure 7. Reverse recovery of Ga_2O_3 rectifiers before and after gamma irradiation. Rectifier was switched from +3 V to −5 V for the reverse recovery characteristics measurements.

Conclusions

^{60}Co gamma–ray irradiation of Ga_2O_3 rectifiers shows that this material has high intrinsic radiation hardness, with minimal changes in rectifier characteristics up to absorbed doses of 100kGy(Si). The changes induced by gamma-ray exposure are much smaller than caused by proton, electron, alpha particle and neutron damage in the same rectifier structures, which allows a direct comparison of these effects since there are no changes in device type, layer thickness or doping. While our work is still somewhat preliminary and more work is needed to understand the trap levels induced by gamma-irradiation, their thermal stability, the effect on carrier lifetime and how different gate oxides in MOS structures respond, the results do show that Ga_2O_3-based devices deployable in space or high radiation terrestrial applications, such as solar blind UV photodetectors and power electronics should have excellent tolerance to gamma ray fluences. The changes in carrier concentration at the doses we employed are small enough that the rectifier properties do not degrade very much.

Acknowledgments

The work at UF is partially supported by HDTRA1-17-1-0011 (Jacob Calkins, monitor). The project or effort depicted is sponsored by the Department of the Defense, Defense Threat Reduction Agency. The content of the information does not necessarily reflect the position or the policy of the federal government, and no official endorsement should be inferred. The work at Korea University was supported by Space Core Technology Development Program (2017M1A3A3A02015033) and the Technology Development Program to Solve Climate Changes (2017M1A2A2087351) through the National Research Foundation of Korea funded by the Ministry of Science, ICT and Future Planning of Korea. D.J.S. acknowledges the use of facilities in the John M. Cowley Center for High Resolution Electron Microscopy at Arizona State University.

ORCID

Chaker Fares https://orcid.org/0000-0001-9596-2381
F. Ren https://orcid.org/0000-0001-9234-019X
S. J. Pearton https://orcid.org/0000-0001-6498-1256
Jihyun Kim https://orcid.org/0000-0002-5634-8394

References

1. F. Nava, A. Castaldini, A. Cavallini, P. Errani, and V. Cindro, *IEEE Trans. Nucl. Sci.*, **53**, 2977 (2006).
2. F. Moscatelli, A. Scorzoni, A. Poggi, M. Bruzzi, S. Sciortino, S. Lagomarsino, G. Wagner, I. Mandic, and R. Nipoti, *IEEE Trans. Nucl. Sci.*, **53**, 1557 (2006).
3. Shinobu Onoda, Takeshi Ohshima, Toshio Hirao, Kenta Mishima, Shigeomi Hishiki, Naoya Iwamoto, Kazuhisa Kojima, and Katsuyasu Kawano, *IEEE Trans. Nucl. Sci.*, **54**, 1953 (2007).
4. S. Onoda, N. Iwamoto, S. Ono, S. Katakami, M. Arai, K. Kawano, and T. Ohshima, *IEEE Trans. Nucl. Sci.*, **56**, 3218 (2009).
5. A. Ionascut-Nedelcescu, C. Carlone, A. Houdayer, H. J.von Bardeleben, J.-L. Cantin, and S. Raymond, *IEEE Trans Nucl. Sci*, **49**, 2733 (2002).
6. Alexander Y. Polyakov, S. J. Pearton, Patrick Frenzer, Fan Ren, Lu Liu, and Jihyun Kim, *J. Mater. Chem. C*, **1**, 877 (2013).
7. S. J. Pearton, Richard Deist, Fan Ren, Lu Liu, Alexander Y. Polyakov, and Jihyun Kim, *J. Vac. Sci. Technol.*, **A31**, 050801 (2013).
8. G. A. Umana-Membreno, J. M. Dell, T. P. Hessler, B. D.Nener, G. Parish, L. Faraone, and U. K. Mishra, *Appl. Phys. Lett.*, **80**, 4354 (2002).
9. G. A. Umana-Membreno, J. M. Dell, G. Parish, B. D. Nener, L. Faraone, and U. K. Mishra, *IEEE Trans. Electr. Dev.*, **50**, 2326 (2003).
10. S. A. Vitusevich, A. M. Kurakin, R. V. Konakova, A. E. Belyaev, and N. Klein, *Appl. Surf. Sci*. **255**, 784 (2008).
11. J. Lee, A. Yadav, M. Antia, V. Zaffino, E. Flitsiyan, L. Chernyak, J. Salzman, B. Meyler, S. Ahn, Fan Ren, and S. J. Pearton, *Rad Eff. Defects Solids*, **172**, 250 (2017).
12. O. Aktas, A. Kuliev, V. Kumar, R. Schwindt, S. Toshkov, D. Costescu, J. Stubbins, and I. Adesida, *Solid-State Electronics*, **48**, 471 (2004).

13. S. A. Vitusevich, A. M. Kurakin, R. V. Konakova, A. E. Belyae, and N. Klein, *Appl. Surf. Sci.*, **255**, 784 (2008).
14. Y.-H. Hwang, Yueh-Ling Hsieh, Lei Lei, Shun Li, Fan Ren, S. J. Pearton, Anupama Yadav, C. Schwarz, M. Shatkhin, L. Wang, E. Flitsiyan, L. Chernyak, A. G. Baca, A. A. Allerman, and Carlos A. Sanchez, *J. Vac. Sci. Technol. B*, **32**, 031203 (2014).
15. C. Inguimbert and S. Messenger, *IEEE Trans. Nucl. Sci.*, **59**, 3117 (2012).
16. E. El Allam, C. Inguimbert, A. Meulenberg, A. Jorio, and I. Zorkani, *J.Appl. Phys*, **123**, 095703 (2018).
17. M. A. Xapsos, G. P. Summers, C. C. Blatchley, C. W. Colerico E.A. Burke, S. R. Messenger, and P. Shapiro, *IEEE Trans. Nucl. Sci.*, **41**,1945 (1994).
18. E. El Allam, C. Inguimbert, T. Nuns, A. Meulenberg, A. Jorio, and I. Zorkani, *IEEE Trans. Nucl. Sci.*, **64**, 991 (2017).
19. J. R. Srour, C. J. Marshall, and P. W. Marshall, *IEEE Trans. Nucl. Sci.*, **50**, 653 (2003).
20. G. P. Summers, E. A. Burke, P. Shapiro, S. R. Messenger, and R. J. Walters, *IEEE Trans. Nucl. Sci.*, **40**, 1372 (1993).
21. Jihyun Kim, S. J. Pearton, Chaker Fares, Jiancheng Yang, Fan Ren, Suhyun Kim, and Alexander Y. Polyakov, *J. Mater. Chem. C*, **7**, 10 (2018).
22. S. J. Pearton, J. Yang, P. H. Cary IV, F. Ren, J. Kim, M. J. Tadjer, and M. A. Mastro, *Appl. Phys. Rev.*, **5**, 011301 (2018).
23. E. Farzana, M. Chaiken, T. Blue, A. R. Arehart, and S. A. Ringel, *APL Materials*, **7**, 022502 (2019).
24. S. J. Pearton, Fan Ren, Marko Tadjer, and Jihyun Kim, *J. Appl. Phys.*, **124**, 222901 (2018).
25. Man Hoi Wong, Akinori Takeyama, Takahiro Makino, Takeshi Ohshima, Kohei Sasaki, Akito Kuramata, Shigenobu Yamakoshi, and Masataka Higashiwaki, *Appl. Phys. Lett.*, **112**, 023503 (2018).
26. More details on the epi wafers are given at the Novel Crystal Technology website https://www.novelcrystal.co.jp/eng/products/hvpe/ϕ2-inch .
27. Y. Oshima, E. G. Víllora, and K. Shimamura, *J Cryst Growth*, **410**, 53 (2015).
28. K. Nomura, K. Goto, R. Togashi, H. Murakami, Y. Kumagai, A. Kuramata, S. Yamakoshi, and A. Koukitu, *J. Cryst Growth*, **405**, 19 (2014).
29. Yao Yao, Serdal Okur, A Luke, M. Lyle, Gary S. Tompa, Tom Salagaj, Nick Sbrockey, Robert F. Davis, and Lisa M. Porter, *Mater. Res. Lett.*, **6**, 268 (2018).
30. Xiangqian Xiu, Liying Zhang, Yuewen Li, Zening Xiong, Rong Zhang, and Youdou Zheng, *J. Semiconductors*, **40**, 011805 (2019).
31. K. William, Yunping Xi, and Dan Naus, "A Review of the effects of radiation on microstructure and properties of concretes used in nuclear power plants" U.S.NRC, NUREG/CR7171, ORNL/TM-2013/263 (2013).
32. V. V. Emtsev, V. Yu. Davydov, V. V. Kozlovskii, V. V. Lundin, D. S. Poloskin, A. N. Smirnov, N. M. Shmidt, A. S. Usikov, J. Aderhold, H. Klausing, D. Mistele, T. Rotter, J. Stemmer, O. Semchinova, and J. Graul, *Semiconductor Sc. Technology*, **15**, 73 (2000).
33. J. H. Cahn, *J. Appl. Phys.*, **30**, 1310 (1959).
34. I. Lyubomirsky, M. Rabinal, and D. Cahen, *J. Appl. Phys*, **81**, 6684 (1997).
35. J. H. Hubbell and S. M. Seltzer, Tables of x-Ray Mass Attenuation Coefficients and Mass Energy-Absorption Coefficients 1 KeV to 20 MeV for Elements Z = 1 to 92 and 48 Additional Substances of Dosimetric Interest. NIST, 1995.
36. M. Passlack, N. E. J. Hunt, E. F. Schubert, G. J. Zydzik, M. Hong, J. P. Mannaerts, R. L. Opila, and R. J. Fischer, *Appl. Phys. Lett.*, **64**, 2715 (1994).
37. R. L. Pease, E. W. Enlow, G. L. Dinger, and Paul Marshall, *IEEE Trans. Nucl. Sci.*, **34**, 1140 (1987).
38. Neal D. Reynolds, Cristian D. Panda, and John M. Essick, *Amer. J. Physics*, **82**, 196 (2014).
39. Stephen M. Seltzer, *Radiation Research*, **136**,147 (1993).
40. C. Schwartz, A. Yadav, E. Flitsiyan M.Shatkin, L. Chernyak, V. Kasiyan, L. Liu, Y. Xi, F. Ren, and S. J. Pearton, *Appl. Phys. Lett.*, **102**, 062102 (2013).
41. J. Kim, F. Ren, G. Y. Chung, M. F. MacMillan, A. G. Baca, R. D. Briggs, D. Schoenfeld, and S. J. Pearton, *Appl. Phys. Lett.*, **84**, 371 (2004).
42. C. W. Wang, B. S. Soong, J. Y. Chen, C. L. Chen, and Y. K. Su, *J. Appl. Phys.*, **88**, 6355 (2000).
43. S. J. Pearton, F. Ren, E. Patrick, M. E. Law, and A. Y. Polyakov, *ECS J. Solid State Sci. Technol.*, **5**, Q35 (2016).
44. Max F. Chaiken and Thomas E. Blue, *IEEE Trans. Nucl. Sci.*, **65**, 1147 (2018).
45. A. Y. Polyakov, N. B. Smirnov, I. V. Shchemerov, E. B. Yakimov, S. J. Pearton, Chaker Fares, Jiancheng Yang, Fan Ren, Jihyun Kim, P. B. Lagov, V. S. Stolbunov, and A. Kochkova, *Appl.Phys.Lett.*, **113**, 092102 (2018).
46. A. Y. Polyakov, N. B. Smirnov, I Shchemerov, S. J. Pearton, Fan Ren, A. Chernykh, P. B. Lagov, and Timur V. Kulevoy, *APL. Mater.*, **6**, 096102 (2019).
47. Jiancheng Yang, Chaker Fares, Yu Guan, F. Ren, S. J. Pearton, Jinho Bae, Jihyun Kim, and Akito Kuramata, *J.Vac. Sci. Technol. B.*, **36**, 031205 (2018).
48. J. D. Lee, Elena Flitsiyan, Leonid Chernyak, Jiancheng Yang, Fan Ren, S. J. Pearton, Boris Meyler, and Y. Joseph Salzman, *Appl. Phys. Lett.*, **112**, 082104 (2018).
49. A. Y. Polyakov, N. B. Smirnov, I. V. Shchemerov, E. B. Yakimov, Jiancheng Yang, F. Ren, Gwangseok Yang, Jihyun Kim, A. Kuramata, and S. J. Pearton, *Appl. Phys. Lett.*, **112**, 032107 (2018).
50. J. Yang, Zhiting Chen, F. Ren, S. J. Pearton, Gwangseok Yang, Jihyun Kim, Jonathan Lee, Elena Flitsiyan, Leonid Chernyak, and A. Kuramata, *J. Vac. Sci. Technol. B*, **36**, 011206 (2018).
51. G. Yang, S. Jang, F. Ren, S. J. Pearton, and J. Kim, *ACS Appl. Mater. Interfaces*, **9**, 40471 (2017).
52. J. Yang, F. Ren, S. J. Pearton, G. Yang, J. Kim, and A. Kuramata, *J. Vac. Sci. Technol. B*, **35**, 031208 (2017).